The Journal of Engine Research

Journal Homepage: www.engineresearch.ir

Numerical simulation of in-cylinder tumble flow field measurements and comparison to experimental results

A. Mohammadebrahim[1], B. Shafiei[2], S. Kazemzadeh Hannani[3*]

[1]*Sharif University of Technology and Irankhodro Powertrain Company (IPCO), Tehran, Iran, m_ebrahim@ip-co.com*
[2]*Sharif University of Technology, Tehran, Iran, behshad@sharif.edu*
[3]*Sharif University of Technology, Tehran, Iran, hannani@sharif.edu*
[*]*Corresponding Author, Phone Number: +98-912-3018408*

ARTICLE INFO

Article history:
Received: 22 September 2012
Accepted: 08 April 2013

Keywords:
Tumble
Intake port
Gas exchange
Flowbench test
Flow coefficient

ABSTRACT

This paper presents a comparison between measured and predicted results of the in-cylinder tumble flow and the flow coefficient generated by a port-valve-liner assembly on a steady-flow test bench. In this study, computational fluid dynamics (CFD) methods were employed to gain further insight into characteristics of an engine. The purpose was to advance understanding of the stationary turbulence process via computational techniques, at the same time. A simultaneous computer simulation was carried out to predict the in-cylinder flow field of the same engine under the same operating condition, using the Fluent software. The tumble ratio and the flow coefficient from both the numerical simulation and the experimental measurement were compared. A reasonably good level of the agreement has been achieved. Finally, this paper provides a useful validation study for a range of turbulence models for the in-cylinder flow and shows the rate of the tumble flow dispersion in the cylinder.

1) Introduction

Improvements in computer processing power and fluid simulation codes have resulted in rapid advancements in computer-based engine simulation. The use of three-dimensional CFD codes allows for greater understanding of flow dynamics in the parts of gas exchange system, before any prototypes are ever manufactured [1]. In fact, many manufacturers are routinely utilizing CFD as part of their engine design process [2-3]. Steady-state CFD simulation comparison with steady-state flow bench results has been widely applied in academic and industrial research. Many researchers have focused on the improvements of volumetric efficiency, tumble ratio, and swirl ratio [4]. Guy et al. [5] used the commercial CFD package Fluent to complement the traditional optimization strategies. They studied a racing car's flow coefficient using both CFD simulation and experiment. A comparison of results between a CFD prediction and a flow bench measurement demonstrated the validity and usefulness of this approach.

Extensive investigations have been reported on the subject of validation of the CFD codes with the flow field measurements of internal combustion engines [6]. While experimental techniques can render acceptable parameter sensitivity results [7-9], such approach is exhaustive, expensive and time consuming. Both experimental and numerical methods still have a long way to be improved from the academic viewpoint. Nevertheless, for industrial applications, they are useful design tools, provided that the errors are within acceptable limits. The results of experimental investigations are global flow parameters, describing flow coefficient and swirl and tumble intensity. The ongoing progress for the development of CAE tools has led to the creation of new methodologies. CFD calculations provide insight into the details of port and in-cylinder flow, thus enabling efficient optimization.

In the present study, numerical simulations are done with tumble adaptor to have similarity between simulation and experimental test, while previous studies ignored this adaptor. However others just use one or two turbulence model(s), in this study, different turbulence models is applied and compared. Finally swirl/tumble are calculated and presented in some planes that will be useful to study swirl/tumble from top to piston surface.

2) Experimental apparatus

The flow-bench experiments are performed to quantify the in-cylinder tumble motion and engine volumetric efficiency by using the same cylinder head and valve. The experimental set up is shown in Figure 1 schematically. Special mechanisms and fixtures (1) are used to adjust valves lift. In standard tests on engines with four valves per cylinder, inlet or outlet valves are open simultaneously. Test is performed on cylinder head or flow box (2) and a dummy cylinder (3) is used with a diameter equal to engine bore. Pressure drop is measured with a pressure transducer (4) relative to atmospheric pressure. A barometer (7) is used to determine the pressure drop in orifice (8) and consequently to measure the volume flow rate. Desired differential pressures are supplied with a bypass valve (10) and air flow temperature is measured using a thermocouple (11) for air mass flow rate correction.

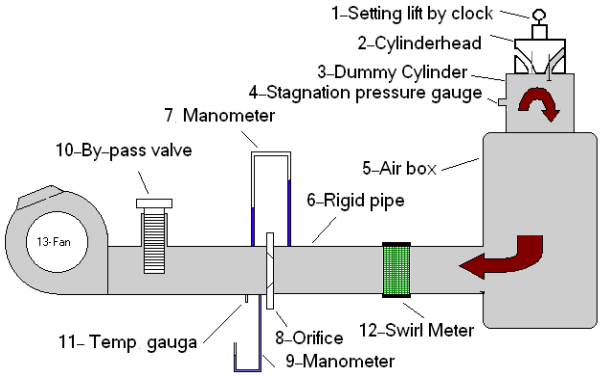

Figure 1: Schematic of flow bench setup [10]

The motor (13) is used in two modes: 1) suction mode which is used to study intake parts e.g. intake manifold and intake port. In this mode, air is sucked from ambient to simulate actual state in engine 2) blowing mode which is used to study outlet parts e.g. exhaust manifold and catalyst convertor. In this mode, air is blown to ambient to simulate actual state in engine. Swirl meter (12) measures tumble and/or swirl intensity, based on its orientation.

The standard test for inlet port consists of measuring the flow coefficient, swirl and tumble intensities for different valve lift. In this test, after applying the desired differential pressure, the valves lift is set at certain level (Figure 2).

Figure 2: valve lift adjustment by the relevant fixtures and dial indicator in the flowbench

Generally, swirl meter measures rotational speed of paddle wheel (because of inlet air flow) as intensity of swirl or tumble (Figure 3(a)), or as shown in Figure 3(b) a torque can be applied from the air to a honeycomb to take into account the intensity of the swirl or tumble. If swirl meter is used with an adaptor like Figure 1, tumble flow is measured and if it is used in orientation like Figure 3, swirl flow is measured.

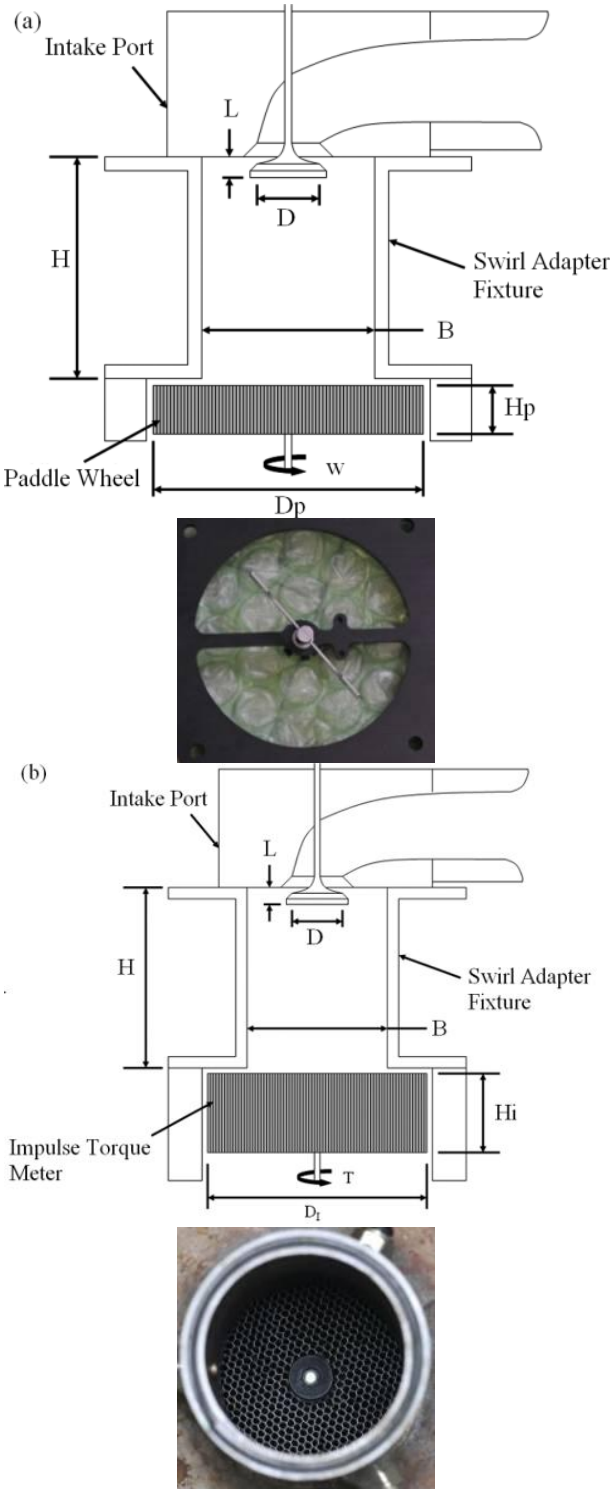

Figure 3: Swirl meter types (a) rotational speed measurement (b) torque measurement [11]

3) Governing Equations and Relations

Using air as the working flow and neglecting body force, the governing equation for homogeneous, compressible, Newtonian fluid include continuity, momentums and *k-ε* equations. These equations are fully described in the literature [12].

The flow and discharge coefficient are defined as the ratio of the experimentally obtained mass flow rate $\dot{m}_{meas}$ to the theoretical mass flow rate $\dot{m}_r$.

$$C_f = \frac{\dot{m}_{meas}}{\dot{m}_r} \tag{1}$$

If the flow is subsonic, the reference mass flow rate is given by

$$\dot{m}_r = A_{ref} \frac{p_0}{\sqrt{RT_0}} \left(\frac{p_T}{p_0} \right)^{1/\gamma} \tilde{p} \tag{2}$$

$$\tilde{p} = \left\{ \left(\frac{2\gamma}{\gamma - 1} \right) \left[1 - \left(\frac{p_T}{p_0} \right)^{(\gamma-1)/\gamma} \right] \right\}^{1/2} \tag{3}$$

While, if the flow is choked, the mass flow is calculated as follows:

$$\dot{m}_r = A_{ref} \frac{p_0}{\sqrt{RT_0}} \gamma^{1/2} \left(\frac{2}{\gamma + 1} \right)^{(\gamma+1)/[2(\gamma-1)]} \tag{4}$$

When the intake phase is analyzed, p_0 is the intake system pressure, p_T is the cylinder pressure, T_0 is the intake system temperature and A_{ref} is the reference area.

The difference between the discharge and flow coefficient lies in the definition of the reference area A_{ref}.

For the discharge coefficient, this area is the valve curtain area and, therefore, it is a linear function of valve lift L_v.

$$A_{ref} = \pi D_v L_v \tag{5}$$

For the flow coefficient, the reference area is given by the cylinder bore:

$$A_{ref} = \frac{\pi B^2}{4} \tag{6}$$

Finally, the flow coefficient is the most common method for assessing the flow efficiency of a port design. The flow coefficient is a non-dimensional parameter that essentially scales the flow rate obtained through a restriction by the theoretical maximum flow rate possible at the restriction's cross-sectional area.

In order to compare the numerical and experimental results, the speed of each node was converted to the volume-average angular momentum:

$$T = \int_0^a |U| U \rho x dA \tag{7}$$

where T is tumble torque (N.m), U is velocity axial to the cylinder (m/s), ρ is density (kg/m^3), x is distance

from axis of rotation (m), a is area of the plane (m^2) and A is area (m^2).

4) Computer Simulation

Computer simulation of the steady flow test for the same engine (Table 1) was conducted on a workstation using Fluent 13. Because of symmetry in cylinder head, half model is used. The parameters used in the problem set-up are listed in Table 2.

The boundary conditions for the model are selected to mimic the conditions of the steady-state flowbench. That is, the pressure gradient across the intake and outlet of the system were specified. The inlet flow into the mesh was confined to be normal to the boundary. Most of the results shown in this paper used a pressure drop of 5.0 kPa, which is commonly used for flowbench testing of conventional engines.

Table 1: Specifications of the EF7-NA engine

General data	bore (mm)	78,6
	stroke (mm)	85
	displacement (cc)	1650
	inlet port diameter (mm)	27
Intake valve	diameter (mm)	30.6
	stem diameter (mm)	6
	maximum lift (mm)	10
	seat angle (deg)	44.5
	inclination (deg)	26

Table 2: Problem set-up

Function	Setting
solver	steady
temporal discretization	implicit
pressure discretization	2nd order upwind
momentum discretization	2nd order upwind
pressure-velocity coupling	PISO
energy discretization	2nd order upwind
turbulence modeling	RNG k-ε
near wall treatment	sta. wall function
fluid model	air (ideal gas)

It should be mentioned that a grid-independence study was performed on this model. Starting with the coarsest grid that could be meshed successfully, and examining progressively finer grids, the predicted C_f for a valve lift of 8 mm were compared. Figure 4 shows that the 99500 tetrahedral cells produced very similar results to the finer grids. This mesh size was used for the remainder of the study.

Steady-state computation was performed. The valve position was kept constant in the simulation.

Reshaping of the grid structure near the interface between the valve seat and the dome cylinder head was performed. Figure 5 shows the final product of grid generation of the port-valve-liner-adaptor assembly with the dome cylinder head.

The grid is denser in the top region, because the flow is expected to be more complicated in this area.

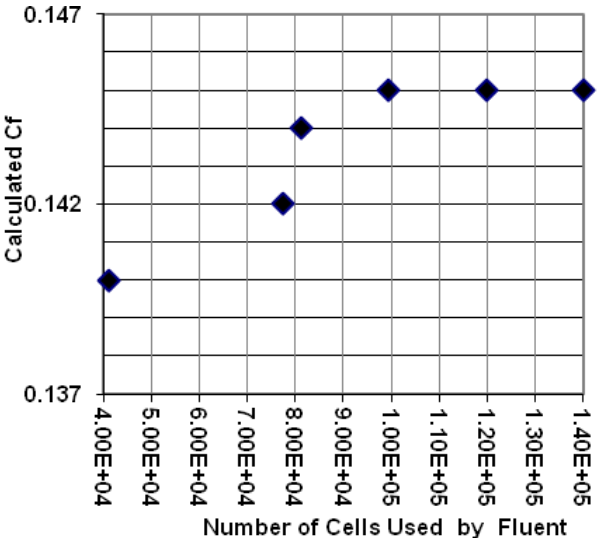

Figure 4: Calculated C_f at Lift = 8mm for various meshing grid sizes

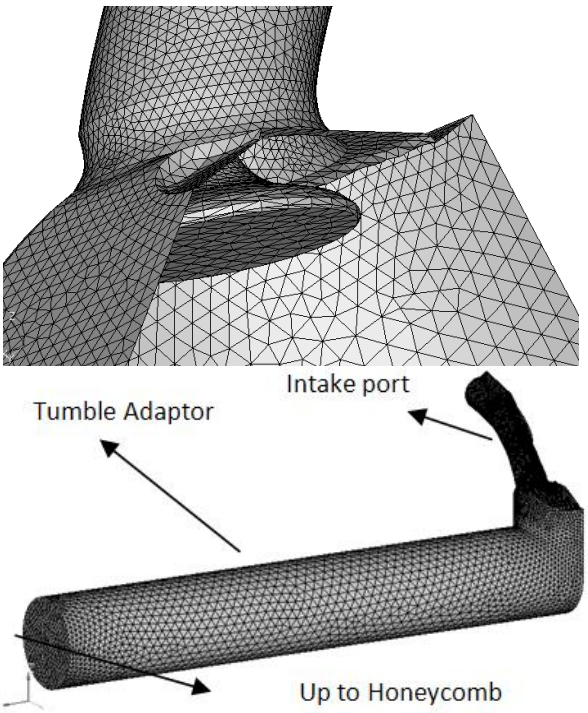

Figure 5: Computational grids of the port-valve-liner assembly with dome-shaped combustion chamber and Intake valve seats

In CFD calculations seven different turbulence models have been applied including RSM model. As it is shown in Figure 6, average vorticity magnitude in cylinder and mass flow rate at outlet are independent of model. These parameters are normalized with maximum values. Maximum difference is 1% in mass flow rate and 9% in vorticity. Also, for more exploration, 10 planes with 10 mm distance are defined (Figure 7) and swirl/tumble torques are calculated and compared versus different turbulence models (Figure 8). Finally, the RNG k-ε turbulence model which

performed more robust for this problem is used with default wall functions. The steady inflow and outflow rates need at least 15000 computational cycles to converge.

In summary, based on the computational results, this problem is independent of turbulence model employed.

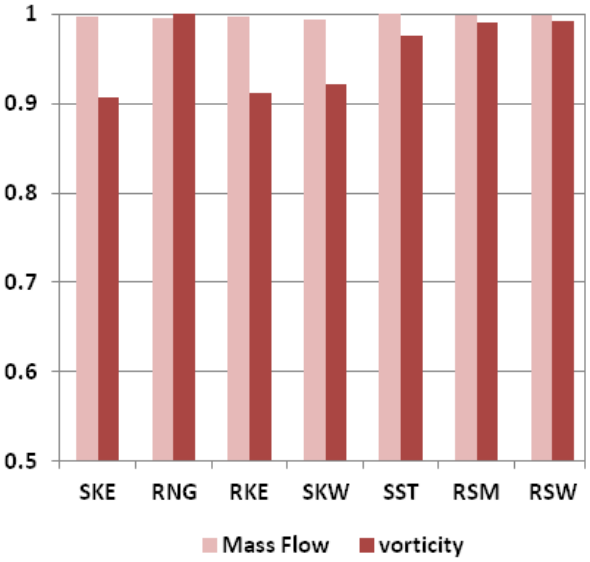

Figure 6: Comparison of normalized mass flow and vorticity for different turbulence models (normalized by maximum of each quantity)

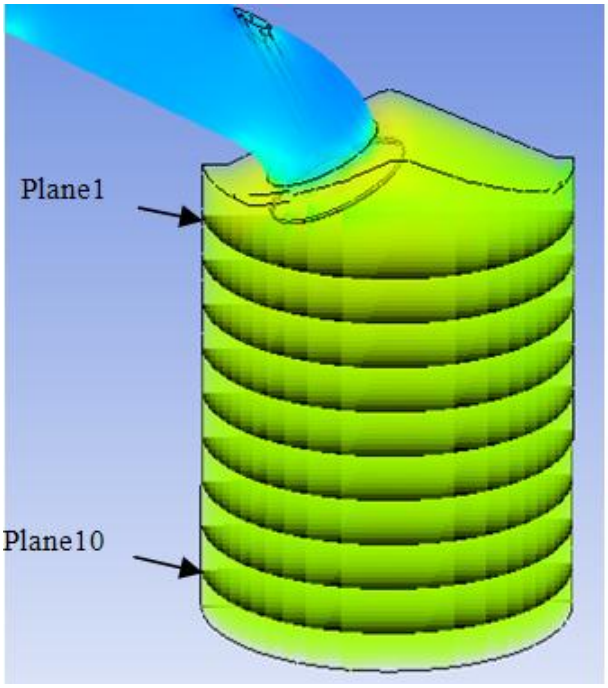

Figure7: Ten planes with 10 mm distance for swirl/tumble torque calculation

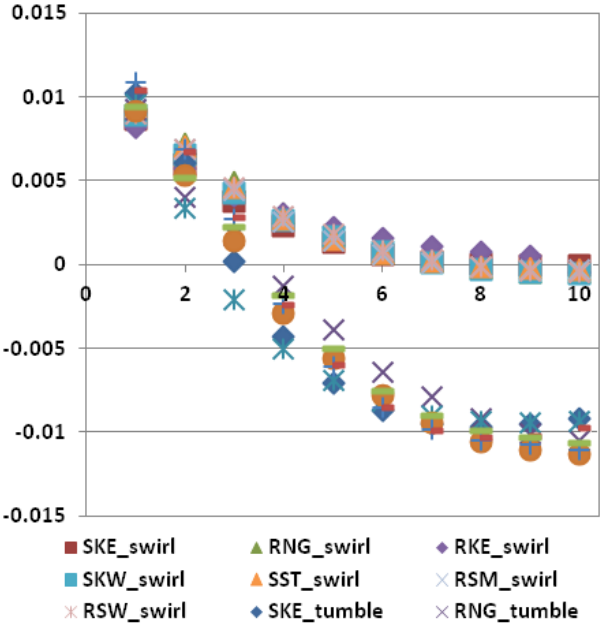

Figure 8: Comparison of swirl/tumble torque (N.m) versus plane number for different turbulence models

5) Simulation Results and Comparison

A comparison of C_f predicted with the CFD model to the C_f measured on a flowbench is shown in Figure 9. The predicted and measured C_f trends are quite similar which provides more confidence that the CFD model is able to replicate the main flow trends within the intake system.

A benefit of using CFD to analyze the intake flow is that it is now possible to examine the detailed behavior of the intake flow at any location within the port, head, or cylinder.

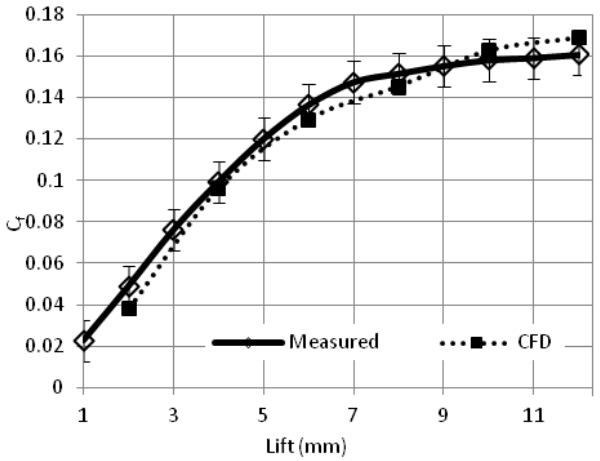

Figure 9: Calculated and Measured Flow Coefficient

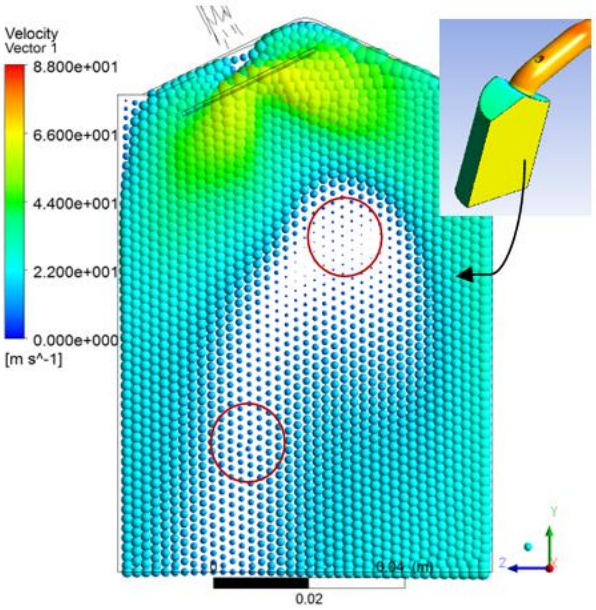

Figure: 10 Computed velocity vector diagrams in the YZ plane (symmetry plane and parallel to cylinder axis)

The simulation results are illustrated by velocity vector diagrams, as displayed in Figures 10 and 11. They are the cross sections on the YZ, and XY planes, respectively. Figure 10 reveals that there are two tumble jets inside the cylinder, one is the main jet with a large vortex guided by the dome chamber; the other is a counter rotating jet with much smaller scale. The maximum velocity is located around the inlet valve curtain. Note that the vectors point downwards at the BDC, because the piston was replaced by the outflow boundary. Figure 11 shows the velocity vector diagram in three horizontal planes. They located at 10 mm, 20 mm, and 30 mm beneath the TDC. With different scales, the flow patterns show similarities in different locations. The flow field tends to be more homogeneous as the flow further downwards.

(a)

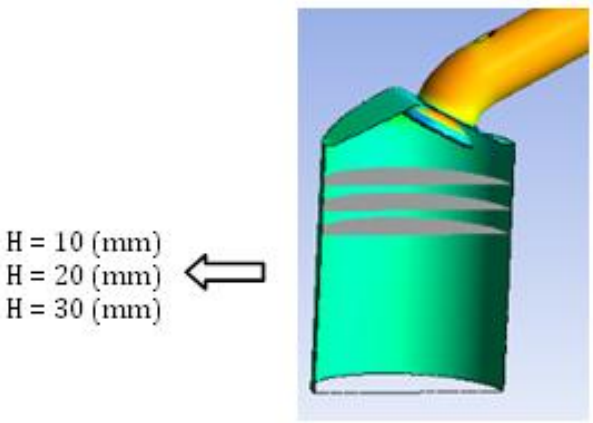

Figure 11: Computed velocity vector diagrams in XY planes, which are located at (b) 10 mm, (c) 20 mm and (d) 30 mm beneath TDC, respectively (Planes are parallel to piston plane and because of symmetry just half-planes are shown)

(b)

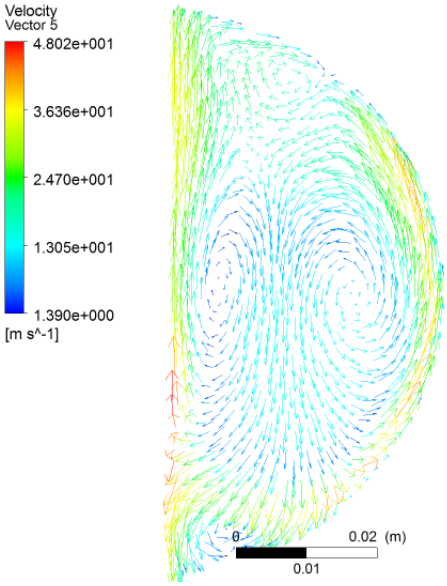

(c)

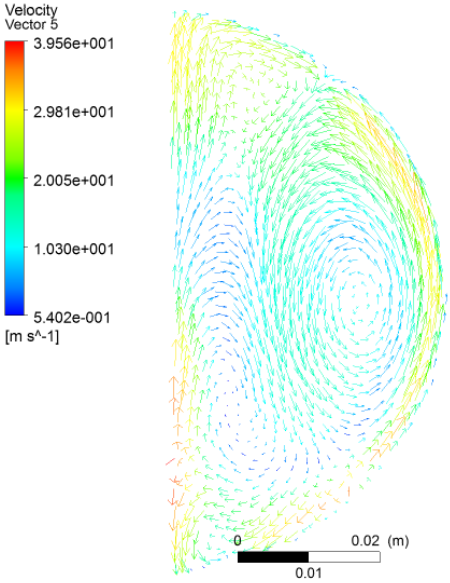

(d)

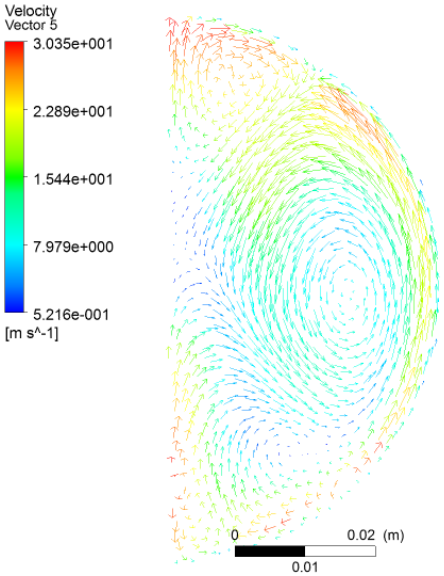

Figure 11 (Continued)

The tumble is shown in Figure 12. The comparison shows that it is in reasonably good agreement between the experimental and simulation results.
The intake flow behavior was found to vary significantly as a function of valve lift. Specifically, it was found that at low lifts the intake flow is relatively uniform around the periphery of the intake port, but at high valve lifts the flow into the cylinder is biased towards the top of the intake port. This results in a tendency to promote tumble at high valve lifts, but not at low valve lifts.
Test is repeated 10 times and error bars indicate uncertainty of each test (Figures 9 and 12). In the flow coefficient measurement, uncertainty is about 1% and in tumble measurement is 3%.

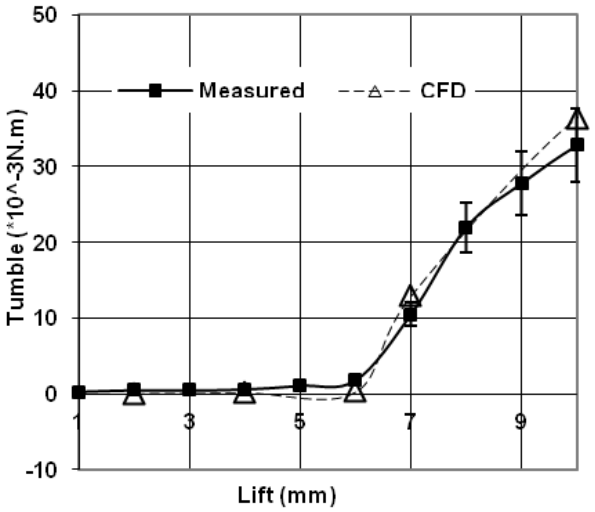

Figure: 12 Comparison of simulation and experimental tumble

6) Conclusion

The flowbench measurement adopted in this research is able to provide accurate quantitative answers. The simulation and experimental results are in reasonable level of agreement. The discrepancy is acceptable to the engine designer. The accuracy is limited by the geometry modeling, CFD limitations, uncertainties of the turbulence modeling and some complex boundary conditions. This paper has validated the engine simulation code, Fluent, in the case of an engine with dome shape combustion CFD provides useful qualitatively information of the flow field in details.
The intake flow behavior was found to vary significantly as a function of valve lift. Specifically, it was found that at low lifts the intake flow is relatively uniform around the periphery of the intake port, but at high valve lifts the flow into the cylinder is biased towards the top of the intake port. This results in a tendency to promote tumble at high valve lifts, but not at low valve lifts.
Finally, this paper provides a useful validation study for a range of turbulence models for the in-cylinder flow and shows rate of tumble flow dispersion in the engine cylinder.

Acknowledgment
Support from CAE department of Irankhodro Powertrain Company (IPCO) is greatly appreciated.

Nomenclature

BDC	Bottom Dead center
TDC	Top Dead Center
CFD	Computational Fluid Dynamics
CAD	Computer Aided Design
RKE	Realizable *k-ε* model
RNG	Renormalization group *k-ε* model
RSM	Reynolds stress Linear model
RSW	Reynolds stress Omega model
SKE	Standard *k-ε* model
SKW	Standard *k-ω* model
SST	Shear-stress transport *k-ω* model
A_{ref}	Reference area
B	Cylinder bore, Swirl adapter fixture bore
C_d	Discharge coefficient
C_f	Flow coefficient
D_v	Inlet valve inner seat diameter
L_v	Valve lift
$\dot{m}_{meas}$	Measured mass flow rate
$\dot{m}_r$	Theoretical mass flow rate
p_0	Intake system pressure
p_T	Cylinder pressure
R	Gas constant
T_0	Intake system temperature
γ	Ratio of specific heat

References

[1] E. Villiers, C. Othmer, Multi-objective adjoint optimization of intake port geometry, SAE International, Paper No. 2012-01-0905, 2012
[2] O. Laget, A. Kleemann, S. Jay, B. Reveille, S. Henriot, Gasoline engine development using CFD, SAE International, Paper No. 2005-01-3814, 2005
[3] H. Toh, R.F. Huang, K.H. Lin, M.J. Chern, Computational study on the effect of inlet port configuration on in-cylinder flow of a motored four-valve internal combustion engine, Journal of Energy Engineering، Vol. 137, No. 4, 2011
[4] R.F. Huang, K.H. Lin, C.N. Yeh, In-cylinder tumble flows and performance of a motorcycle engine with circular and elliptic intake ports, Experimental Fluids, Vol. 46, pp.165-179, 2009
[5] R.K. Guy, B.R. Teipel, R.H. Stanglmaier, Use of computational fluid dynamics (CFD) tools for high-performance engine tuning, SAE International, Paper No. 2006-01-3666, 2006
[6] J.F.L Coz, S. Henriot, P. Pinchon, An experimental and computational analysis of the flow field in a four-valve spark ignition engine-focus on cycle-resolved turbulence, SAE International, Paper No. 900056, 1990

[7] J.W. Son, S. Lee, B. Han, W. Kim, A correlation between re-defined design parameters and flow coefficient of SI engine intake ports, SAE International, Paper No. 2004-01-0998, 2004
[8] D. Ramajo, N. Nitro, In-cylinder flow CFD analysis of a 4-valve spark ignition engine- comparison between steady and dynamic tests, Journal of Engine Gas Turbines and Power, Vol. 132, No. 5, pp. 121-131, 2010
[9] D. Ramajo, A. Zanotti, N. Nigro, In-cylinder flow control in a four-valve spark ignition engine: numerical and experimental steady rig, Proceedings of the Institution of Mechanical Engineers, Part D: Journal of Automobile Engineering, Vol. 225, 2011
[10] H. Bettes, Flow bench applications and techniques, Superflow, 2003
[11] D.M. Heim, J.B. Ghandhi, Investigation of swirl meter performance, Proceedings of the Institution of Mechanical Engineers, Part D: Journal of Automobile Engineering, 2011
[12] T. Du, Z.N. Wu, Mixed analytical/numerical method applied to the high reynolds k-ε turbulance model, Computational Fluids, Vol. 34, No. 1, pp. 97-119, 2005

فصلنامهٔ علمی- پژوهشی تحقیقات موتور

تارنمای فصلنامه: www.engineresearch.ir

شبیه‌سازی عددی اندازه‌گیری جریان گردبادی داخل استوانه و مقایسهٔ آن با نتایج تجربی

ابوالفضل محمدابراهیم[۱]، بهشاد شفیعی[۲]، سیامک کاظم‌زاده حنانی[۳*]

[۱] دانشگاه صنعتی شریف و شرکت تحقیق، طراحی و تولید موتور ایران‌خودرو (ایپکو)، تهران، ایران، m_ebrahim@ip-co.com

[۲] دانشگاه صنعتی شریف، تهران، ایران، behshad@sharif.edu

[۳] دانشگاه صنعتی شریف، تهران، ایران، hannani@sharif.edu

[*] نویسندهٔ مسئول، شمارهٔ تماس: ۰۹۱۲۳۰۱۸۴۰۸

چکیده

در این مقاله، مقایسه‌ای بین نتایج اندازه‌گیری و پیش‌بینی شدهٔ ضریب جریان و جریان گردبادی با محور افقی انجام شد. نتایج در مجموعه‌ای از اجزاء شامل راهگاه- دریچه و استوانه و با استفاده از آزمون جریان پایا بدست آمد. روش‌های دینامیک سیالات محاسباتی بمنظور دریافت دید بهتر از مشخصات جریان و فهم فرآیندهای آشفتگی به کار گرفته شد. با شبیه‌سازی فرآیند واقعی آزمون میز جریان، توسط نرم‌افزار تجاری فلوئنت (Fluent)، سعی شد تا پیش‌بینی مناسبی از رفتار ضریب جریان و جریان گردبادی انجام شود. نتایج شبیه‌سازی و آزمون تجربی، همخوانی مناسبی را با یکدیگر نشان دادند. در ادامه، با استفاده ار الگوهای مختلف آشفتگی، تأثیر آنها بر متغیرهای مورد نظر بررسی گردید و نهایتاً میرایی جریان گردبادی در صفحات مختلف استوانه ارزیابی شد.

اطلاعات مقاله

تاریخچهٔ مقاله:

دریافت: ۰۱ مهر ۱۳۹۱

پذیرش: ۱۹ فروردین ۱۳۹۲

کلیدواژه‌ها:

تبادل گاز

ضریب جریان

راهگاه ورودی

آزمون میز جریان

جریان گردبادی با محور افقی